Gschliefgraben / Traunstein Mt.

(Ivo Baroň, Robert Supper, Edmund Winkler, David Ottowitz, Klaus Motschka, Sirri Seren, Wolfgang Gasperl, Günter Moser, Katharina Heibl)

WGS coordinates: 47°53'1.91"N, 13°49'1.08"E
Site, county: Gmunden, Upper Austria
Type of the slope failure: complicated complex of earthflows, rotational and translational slides, rockfalls, topples and Deep-Seated Gravitational Slope Deformations at different activity stages
Specific area: entire studied area covers about 5 km^2
Volume: the main active landslide of winter 207/08 reached 3.8 million m^3, the DSGSDs have more than 137.4 million m^3
Age: Postglacial, Holocene, recent

The Gschliefgraben site is one of the most prominent and recently studied slope failures in Central Europe. It comprises a large complex of geologically controlled slides, earth flows, topples, rockfalls and Deep-Seated Gravitational Slope Deformations in the "Gschliefgraben" and along the adjacent slopes of the Northern Calcareous Alps. In late November 2007, a slide/earth flow of about 3.8 million m^3 of colluvial mass was reactivated in the central and western parts of the valley (Fig. 1). The maximum displacement velocity was up to 4.7 m/day at the beginning. Consequently, in frame of the first emergency measures, 55 buildings had to be evacuated.

Recently, the Gschliefgraben landslide is a test site of the European FP7 project SafeLand. New techniques have been tested for an effective early warning, consisting of, e.g., complex airborne and ground-based geophysical surveys, and the GEOMON^{4D} (continuous geoelectric) and DMS (automatic inclinometer) monitoring systems.

Figure 1. Aerial photo of the Gschliefgraben Valley and Traunstein Mt. from W (Photo by: R. Supper, 2009)

Geological and Geomorphic settings

The Gschliefgraben is a 2.85 km long and 0.85 km wide valley along the foot of the Northern Calcareous Alps (Fig. 1) south of the town of Gmunden. The front of the Northern Calcareous Alps forms here a steep cuesta with the summit of Mt. Traunstein (1,691 m a.s.l.). The valley is divided into small sub-parallel catchments; its topography is controlled by complicated tectonics and a very complex lithology, as well as by mass wasting that has been active here at least since the end of the last glacial period.

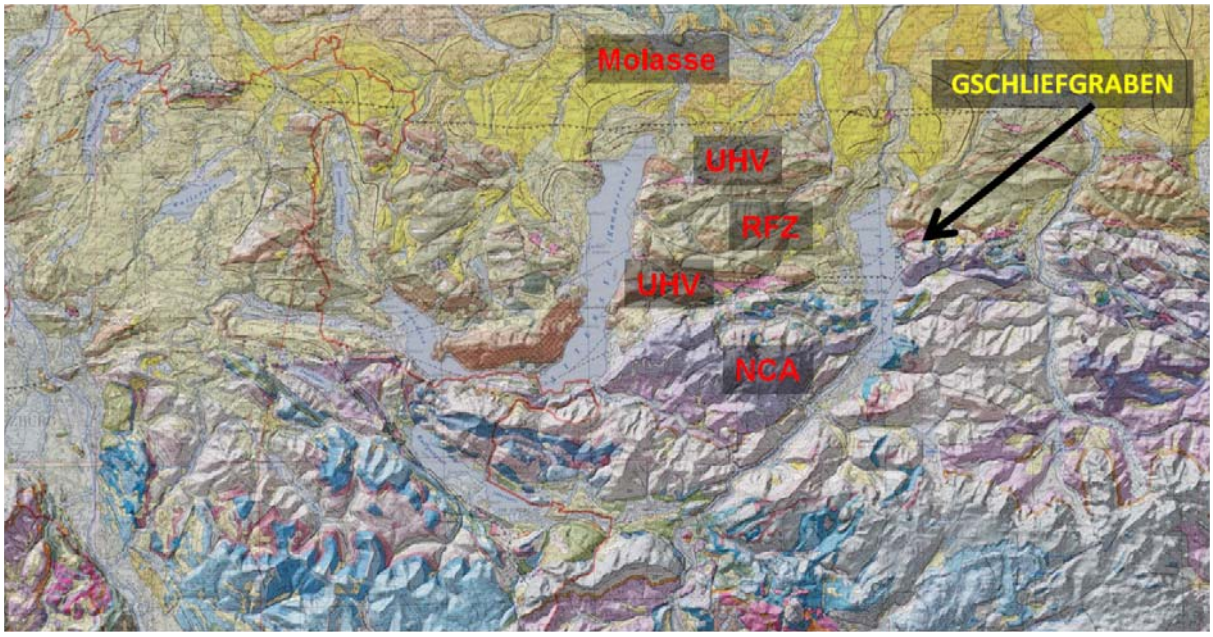

Figure 2. Geological map of the northern part of the Eastern Alps near Gschliefgraben: UHV – Ultrahelveticum, RFZ – Rhenodnubian flysch zone, NCA – Northern Calcareous Alps. The longitudinal extent of the map is about 80 km.

The area covers three main geological units with a completely different lithological and geological structure (Figs. 2, 3, 4, and 5), i.e.: (i) Northern Calcareous Alps and the "Marginal Nappe" (klippen belt) (NCA), (ii) Ultrahelveticum (UHV) and (iii) the Rhenodanubian Flysch Zone (RFZ).
The NCA unit (Triassic-Cretaceous age) is composed of densely fractured, diversely stratified, steeply dipping and frequently faulted competent brittle rocks there. Dolomite and Limestone are the most abundant rock types. The substrate is highly permeable and the joints often have a character of opened cracks.

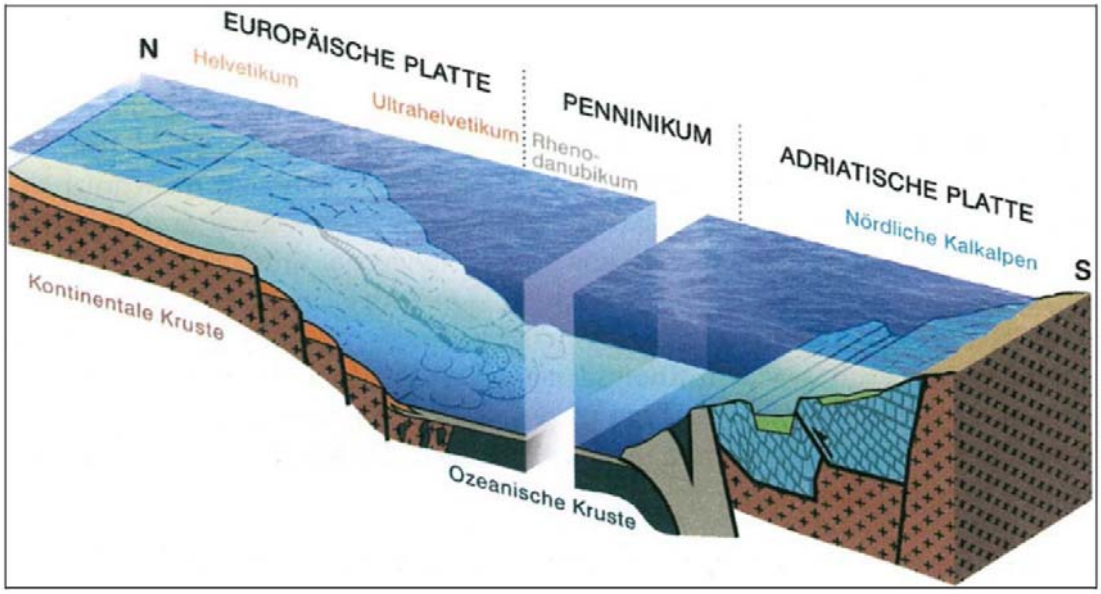

Figure 3. Schematic Late Cretaceous section of the junction of the European and Adriatic plates along their collisional margin approximately at place of the Gsgliefgraben valley (after Egger & Husen Van 2007 in Moser et al. 2011).

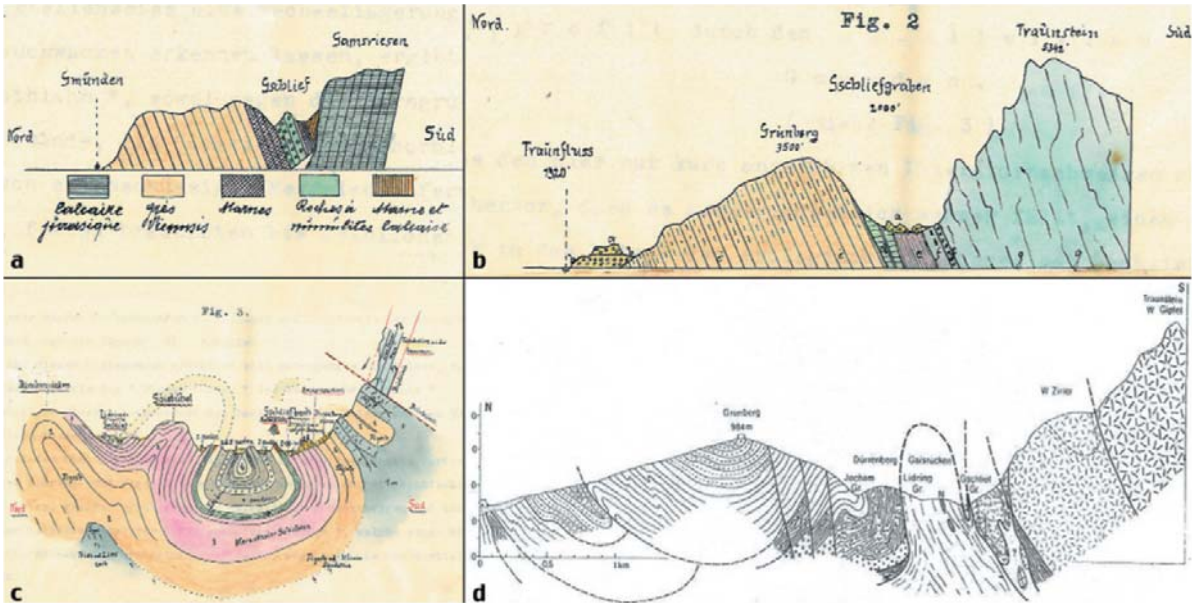

Figure 4. Historical geological sections of the Gschliefgraben valley oriented N-S by different authors: (A) Weg von BOUÉ (1832), (B) Mojsisovics & Schloenbach (1864), and (C-D) Koch (1894) in Weidinger (2009).

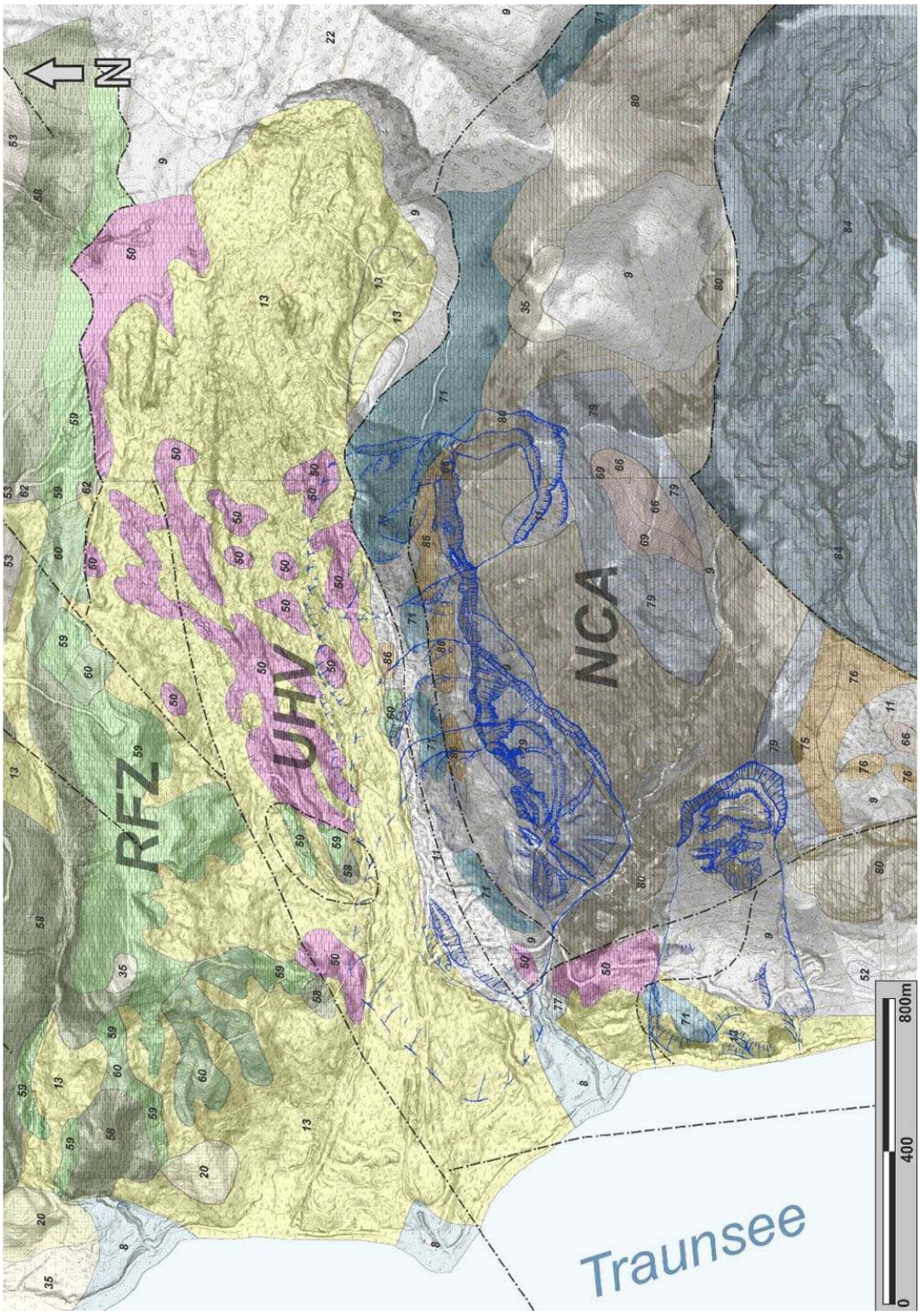

Figure 5. Geological map of the area of Gschliefgraben and surroundings. The blue contours indicate the Deep-Seated Gravitational Slope Deformations. Legend: Quaternary deposits: 8 - Alluvial Fan, 9 - Slope Scree, 11 - Block Fields, 13 - Landslide Deposits, 20 - Glacilacustrine deposits, 22 - Slope Breccia, 35 - Moraine deposit; UHV: 50 - Buntmergel Fm., 52 - Greisten Fm.; RFZ: 53 - Altliengbach Fm., 57 - Perneck Fm., 58 - Zementmergel Fm., 59 - Seiesenburg Fm., 60 - Rieselsberg Fm., 62 - Gaultflysch Fm.; NCA: 66 - Schrambach Fm., 69 - Ruhpolding Fm., 71 - Calcarenite Fm., 75 - Koessen Fm., 76 - Koessen Fm., 77 - Koessen Fm., 79 - Plattenkalk Fm., 80 - Hauptdolomit Fm., 84 - Wetterstein Fm., 85 - Guttenstein Fm., 86 - Haselgebirge Fm.; the major tectonic faults are as dot-and-dashed lines (modified after Egger et al. 1996, Egger et al. 2007 and Moser et al. 2009)

The UHV unit (Cretaceous-Lower Tertiary age) comprises tectonically strongly deformed variegated marl, claystone, nummulitic limestone, sandstone, arcose etc. This unit is the most incompetent one in the study area. The material contains a relatively high fraction of swelling clay minerals. Moreover the soft rocks are intensively tectonically fragmented (Fig. 6). The rocks of the UHV are locally quite permeable (fractured sandstone, limestone etc.), however impermeable zones prevail. Tectonic joints use to be filled with secondary or tectonic clay. Due to these facts, this zone shows a relatively low resistivity, and a high U, K and Th content.
The RFZ (Cretaceous age) is built up mostly with slate, shale, cemented marl and sandstone of different thickness. The alteration of competent vs. incompetent and permeable vs. impermeable rocks exhibit high local contrast resulting in a distinct local contrast of resistivity and U, K, and Th content.

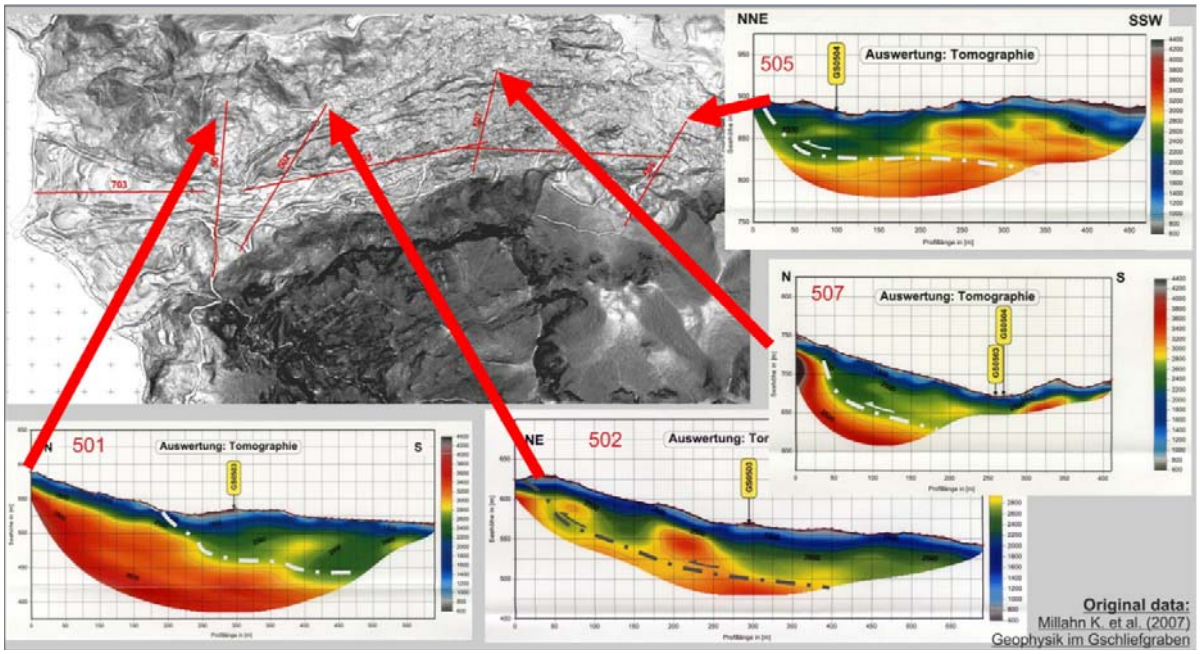

Figure 6. The seismic tomography profiles indicate up to 70 m deep compressional deformation, which could be related to loading of incompetent ultrahelvetic rocks by competent dolomites and limestones of NCA situated tectonically above them (original data Millahn et al. 2007).

Mass wasting processes

The main mass wasting processes are represented by sliding and flowing in the central part (Fig. 7), which is built up mostly of the UHV unit. The UHV emerge here in a form of the tectonic window between the RFZ and the NCA. On the other hand, falling, toppling, and spreading are the most characteristic types of mass movement in the eastern and southern marginal areas of the Gschliefgraben valley along NCA, where hard rock dominates (dolomite, limestone, cemented Pleistocene breccia). At some places, great portions of the NCA and the below situated RFZ and UHV units are subject to Deep-Seated Gravitational Slope Deformations in a rather initial evolution stage (Fig. 5)

Figure 7. The activity of the earthflow complex between 2000 and 2008 assessment was based on the identification of bare surfaces on set of orthophotos. The orthophotos are superimposed on an ALS greyscale slope gradient map.

A set of 5 high-resolution Airborne Laser Scan (ALS) scenes, which were taken at different times in April 2007, January, February, March and September 2008, represented the ground surface topography of Gschliefgraben just before, during, and after the major recent landslide event of winter 2007/08.

The detailed geomorphic analysis of the ALS DTMs and orthophotos enabled (i) to recognize individual slope failures and their deposits and (ii) to distinguish the active slides and earthflows from dormant (inactive) and old ones (Figs. 7, 8, and 9). These observations were compiled in a form of the landslide inventory map (Fig. 10). The mass-movement phenomena in the area include different types of landslides at different volumes, evolutionary stages and activity level, forming a complicated complex. Due to the limited time available, limited scale and complexity of slope failures, the presented inventory could only deal with a rough classification. Shallow and deep-seated slides (slumps), their transitions to earthflows, earthflows alone, fallen boulders or sagged slopes and toppled rock towers were the most abundant landslide types. At relatively large portion of the valley, individual bodies of dormant (inactive) rather small scale earthflows and slumps were not

distinguishable from each other. Thus they were grouped together as the category "5" (Fig. 10). The active slides and earthflows (active between 2000 and 2008) were distinguished well and they had affected about 5 % of the study area (Fig 10).

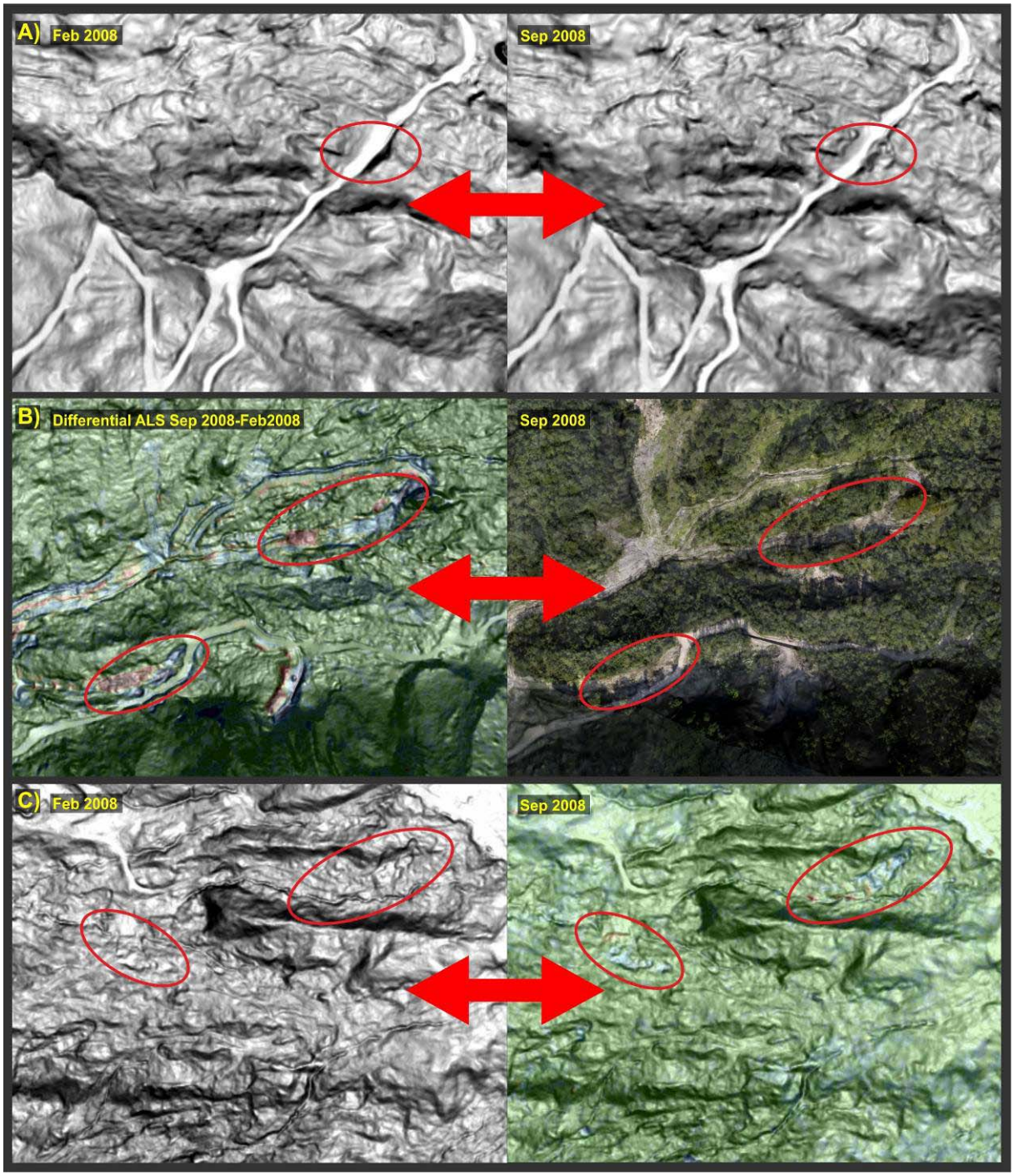

Figure 8. The activity assessment of landslides was based on differential ALS, as evidenced by some examples: A) two separate ALS pseudo-hillshades taken in different time, B) differential ALS model and the orthophoto, and C) pseudo-hillshade and superimposed differential ALS model.

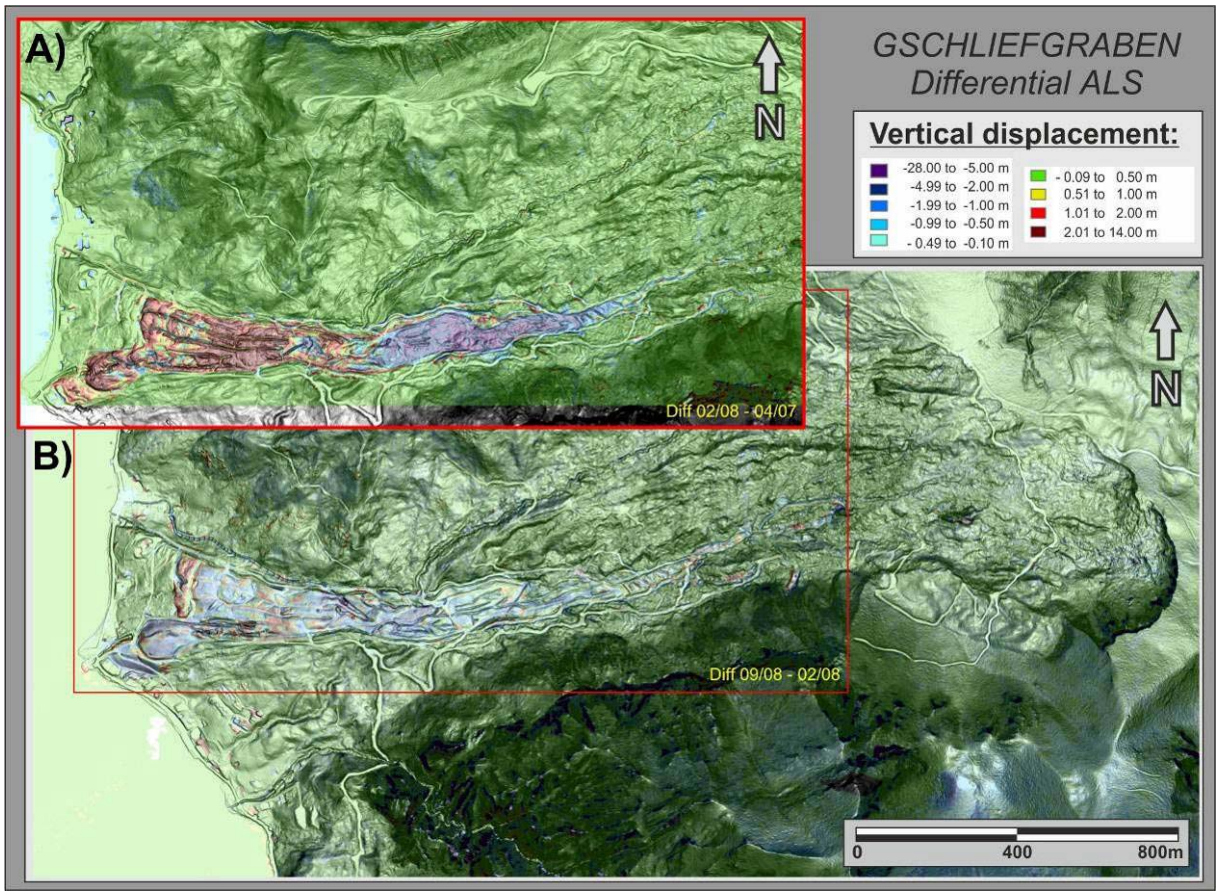

Figure 9. Two differential ALS scenes highlight mass transport due to (A) the major recent landslide event in winter 2007/08 and (B) latter remedial works comprising of distinct material removal from the active earthflow (below). The presented individual ALS surveys took place in April 2007, February 2008 and September 2008.

The major recent landslide event in winter 2007/08 and subsequent remedial works were well documented by the differential ALS. The main recent earthflow mobilized older mass-movement deposit in the central and lower western part of the Gschliefgraben valley. Distinct subsidence in the upper earthflow portion, as well as the uplift of about 14 m in the accumulation zone was identified (Fig. 9A). The remedial works comprised of distinct material removal from the active earthflow, managed by the Austrian Service for Torrent and Avalanche Control Survey (WLV Austria) in spring and summer 2008 (Fig. 9B).

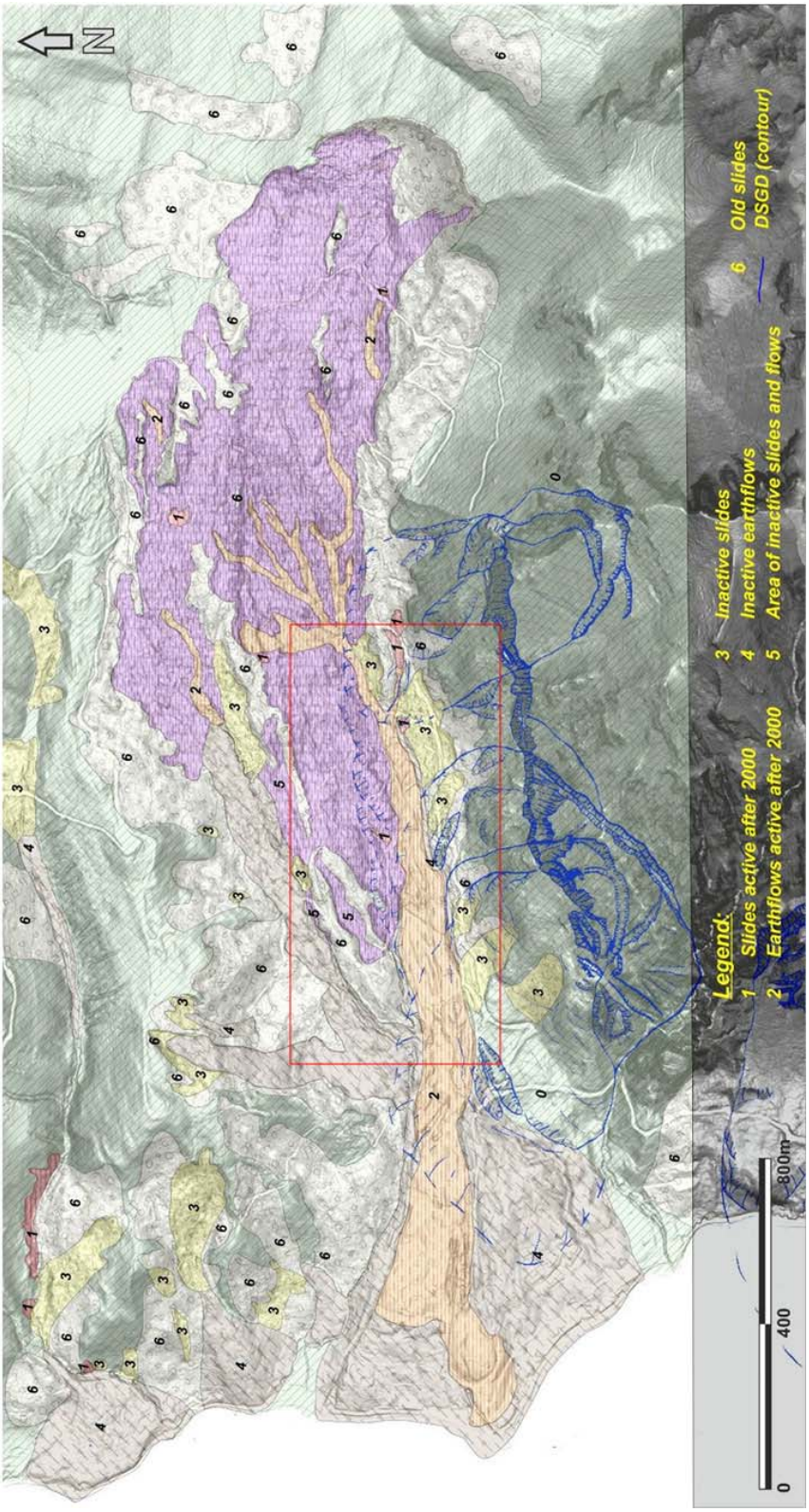

Figure 10. Landslide inventory map of the area of Gschliefgraben. Slope failures comprise more than 50 % of the area, even the Deep-Seated Gravitational Slope Deformations (DSGSD) were not included in the summary.

The slope-failure structure and fabrics

The slope-failure structure and fabrics was investigated mainly by complex geophysical survey, such as: seismic tomography (Millahn et al. 2007, Weidinger 2007), electrical resistivity profiling (Niesner 2008, Supper 2010a), GPR (Seren, not published) and complex helicopter-borne geophysical survey consisting of electromagnetics, gamma-ray and passive-microwave (Supper et al. 2010a, 2010b).

Structures recognized by GPR

Ground-penetrating radar survey performed good information on the shallow situated earthflow structures (Figs. 11 and 12). After post processing (especially migration of the GPR data), individual sheets of recent earthflow accumulations above an in the source area of the 2007/08 landslide were detected, as well as an older buried river channel (Fig. 12).

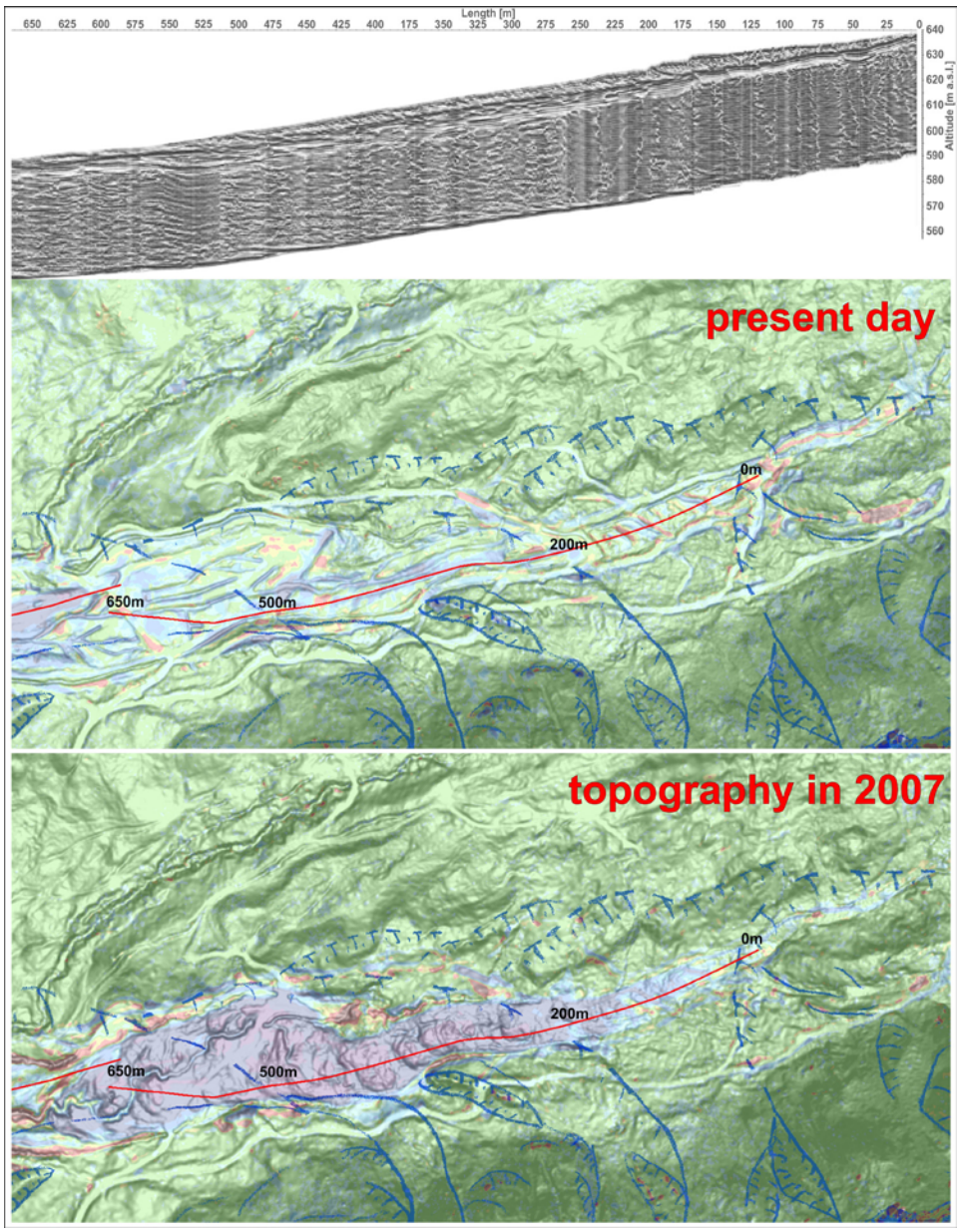

Figure 11. Structure of the subsidence area of the 2007/08 landslide and the upper earthflow accumulations and as seen in GPR profile and two differential ALS DTMs: the uppermost image is a migrated and post-processed GPR profile (provided in 2010 by S. Seren, ZAMG), the middle image shows the profile position on the present-day relief (slope-gradient pseudohillshade) with marked topographic changes after the landslide in 2007/08 (blue=subsidence, yellow/red=accumulation, green=stable, for legend see Fig. 9), and the lower image presents the relief before the landslide event in 2007/08 with marked topographic changes during this event (the blue regions were generally evacuated).

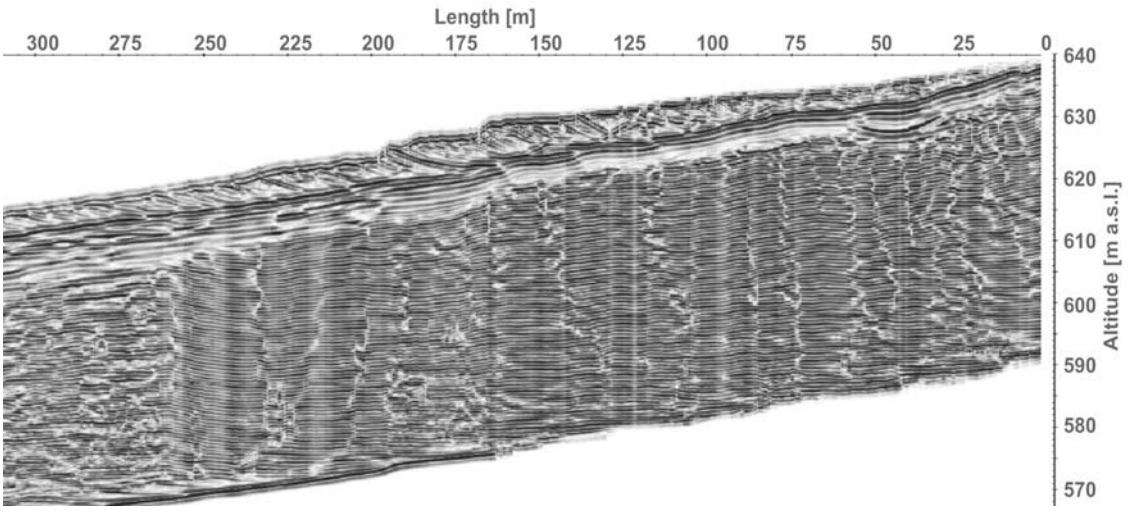

Figure 12. A detail of the internal structure of the upper earthflow accumulations as seen on the migrated and post-processed GPR profile (provided in 2010 by S. Seren, ZAMG).

Structures recognized by the Airborne Electromagnetic survey (HEM)

The subsurface resistivity results show a very distinct pattern differing as well with location and with depth. The central and upper northern parts of the Gschliefgraben valley comprised the areas of the lowest resistivity (Fig. 13). Relatively intermediate values of resistivity prevailed in the western part of the study area and the highest values occurred in the southern, northern and eastern parts. The ground resistivity generally decreased with the depth; only isolated high-resistivity areas occurred in mapped Deep-Seated Gravitational Slope Deformations, and in the NW, NE and SE parts of the study area at the depths below 30 m. However one has to take into account that the very low surface resistivity limits the penetration depth of the electromagnetic system significantly. Consequently no information about structures below can be derived.
The highest resistivity can be contributed to limestone and dolomite rocks, slope scree (and cemented slope breccia) crushed zones and opened cracks in NCA, weathered sandstone and limestone and their colluvium in RFZ. Rather intermediate resistivity occurred in sandstone and nummulitic calcarenite rocks, clayey and stony colluvium in NCA and the main earthflow accumulation. In contrary, the lowest resistivity is typical for major portion of the UHV, which is rich in clay, and for tectonically jointed areas of the RFZ (Fig. 13).

By the 1D multilayer inversion, well confined high resistivity blocks of crushed limestone and dolomite were detected in deep parts on the south. Those blocks correlate well with the mapped Deep-Seated Gravitational Slope Deformations of N slopes of Kaltenbachwildniss / Traunstein (Fig. 14). A rough correlation between the airborne resistivity and the spatial pattern of shallow and intermediate landslides was observed (Fig. 13). The results clearly show that landslides most frequently occurred in the low resistivity zones within the UHV and RFZ. Thus the method could be applicable for defining broader zones which might be susceptible to mass wasting.

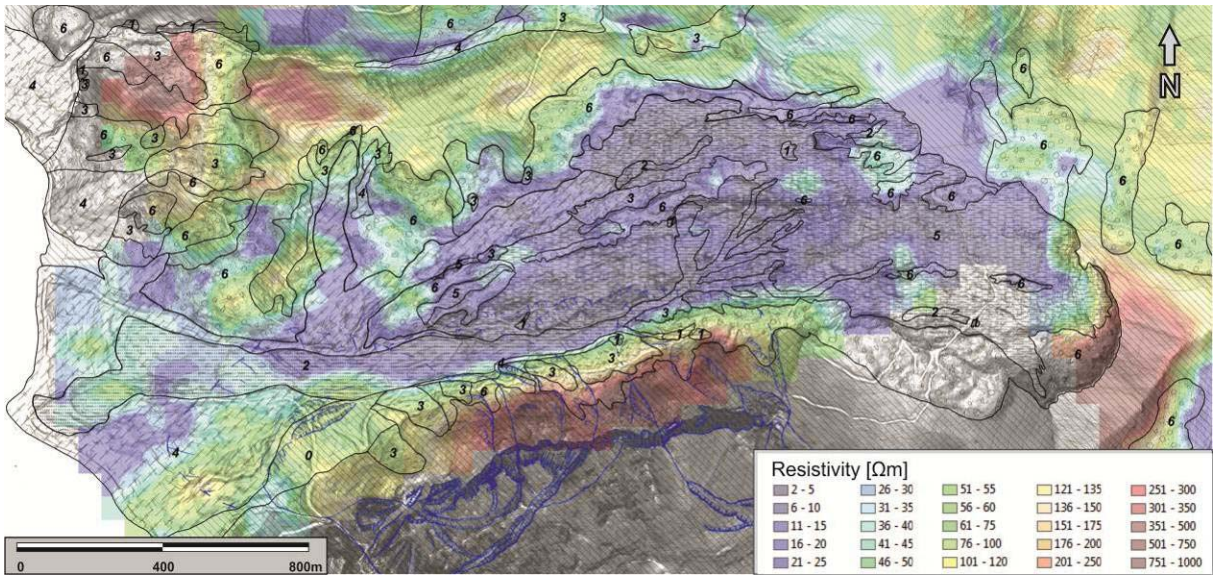

Figure 13. Map of the ground resistivity (homogenous half-space 1+2) at shallow depths compared to the landslide inventory map (Fig. 10). The blue contours define the DSGSDs at northern slopes of Mt. Traunstein.

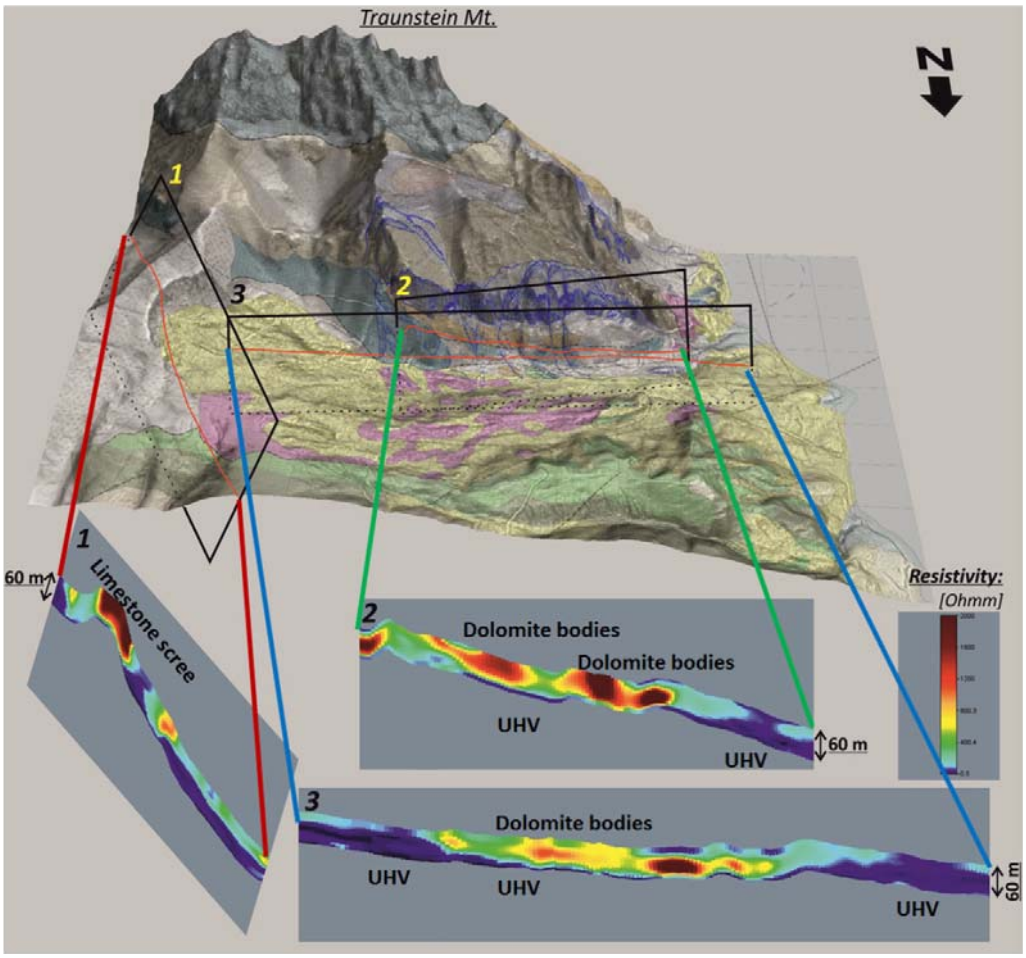

Figure 14. The internal structure of DSGSDs could be seen on helicopter-borne electromagnetic (HEM) cross-sections obtained from the 1D multilayer inversions; the high resistivity dolomitic blocks are sagging into the low-resistivity ultrahelvetic shales, claystones, marls etc. (UHV). The DSGSD contours are in blue, the profiles are marked as red lines on the 3D view of the geological map seen from the N.

Structures recognized by the airborne gamma-ray survey

The airborne gamma-ray survey showed that the content of the radioactive Potassium is related to the original geological structure and landslide pattern (Fig. 15). A low content of Potassium was observed in the southern and eastern portion of the study area. Generally rocks and slope scree of the entire NCA and in the zone of a cemented breccia in SE on the surveyed area, as well as large alluvial fans and the lowermost portion of the Gschliefgraben earthflow exhibit low concentrations, whilst the lowest ones were observed along loosened and crushed limestone, opened cracks as well as along the zones of detachment of the DSGSD. The intermediate or relatively higher Potassium concentrations were observed in the major regions in the centre and in the N of the study area. The highest ones were related to colluvial deposits of inactive dormant or old slides in the RFZ, as well as in the active and dormant slides´/earthflows´ deposits in the UHV. The highest Potassium occurrence most probably correlates with high clay content. High Potassium values can be also found in the upper and middle part of the earthflow indicating that most of its material (at least at the surface) origins from that area. As mentioned above, the lower section of the earthflow shows medium to low Potassium values. From this fact we can conclude that limestone material plays a significant role in the composition of the lower part of the earthflow and/or the low Potassium content was caused by superficial soil removal during the remedial works. The content of Thorium performed similar pattern.

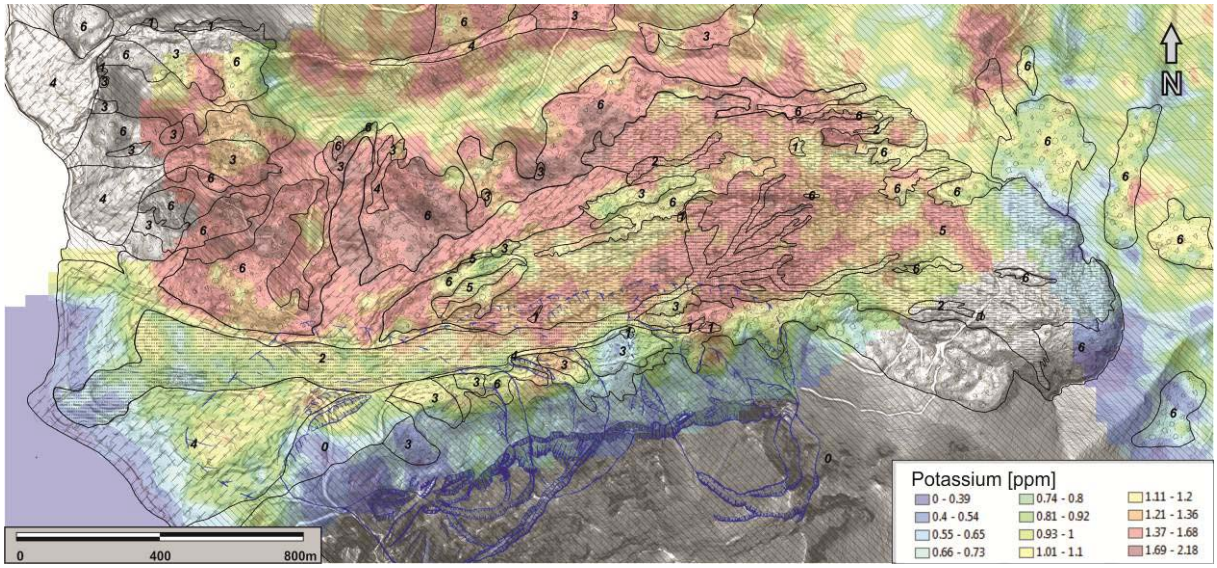

Figure 15. Map of the Potassium content at the ground surface compared to the landslide inventory map. The blue contours define expected extent of the DSGSDs at northern slopes of Mt. Traunstein.

Mass movement mitigation and monitoring

The mitigation works comprised of three different phases. Within the first phase of mitigation in 2008, major measures were focused on property and infrastructure protection. About 220 wells and one deep channel were implemented to drain the sliding mass. Additionally a big quantity of sliding material was removed close to the inhabited areas. Differential GPS and water level measurements were performed to evaluate the effectiveness of the measures, which led to a significant slowdown of the movement. During the second phase (soon after the suspension of the evacuation), multi-disciplinary investigations including drilling, borehole logging and complex geophysical measurements (e.g., geoelectric, seismic and GPR surveys), were performed to investigate the

structure of the landslide area in order to evaluate maximum hazard scenarios as a basis for planning further measures. Based on these results, monitoring techniques for an early warning system are currently being tested within the third phase. This early-warning system should enable local stakeholders to provide an appropriate response in any case of further landslide reactivation.

Figure 16. Location map showing the position of the geoelectric monitoring profiles (red lines) on the landslide of Gschliefgraben

As a part of the early warning approach at the Gschliefgraben test site, a geoelectric monitoring system of the type Geomon^{4D} was installed in the upper central part of the active earthflow of Gschliefgraben in September 2009 (Fig. 16).
The Geomon^{4D} (Fig. 17) was specifically developed for monitoring applications by the Geological Survey of Austria (Supper et al. 2003, 2009, and 2010). The completely open architecture of the instrument allows installation of any number of current or potential electrodes by adding parallel or serial cards. Furthermore, data acquisition at a speed of about 3000 measurements/hour in single channel mode and usually 1000 samples per single configuration including recording of the full signal enable effective noise analysis and filtering. The GPRS (General Packet Radio Service) data transfer allows the maintenance to be performed fully remote-controlled. Data, such as measurement results, test sequences and log files, containing information about system and GPRS connection status are sent automatically via email to the data processing centre at GSA. Consequently, immediate availability of information for local stakeholders could be guaranteed. For power supply a 500 m long cable was installed to connect to the local power grid. The length of the two

perpendicular profiles is 120 m (electrode separation 3 m, 41 electrodes) and 192 m (electrode separation 4 m, 49 electrodes).

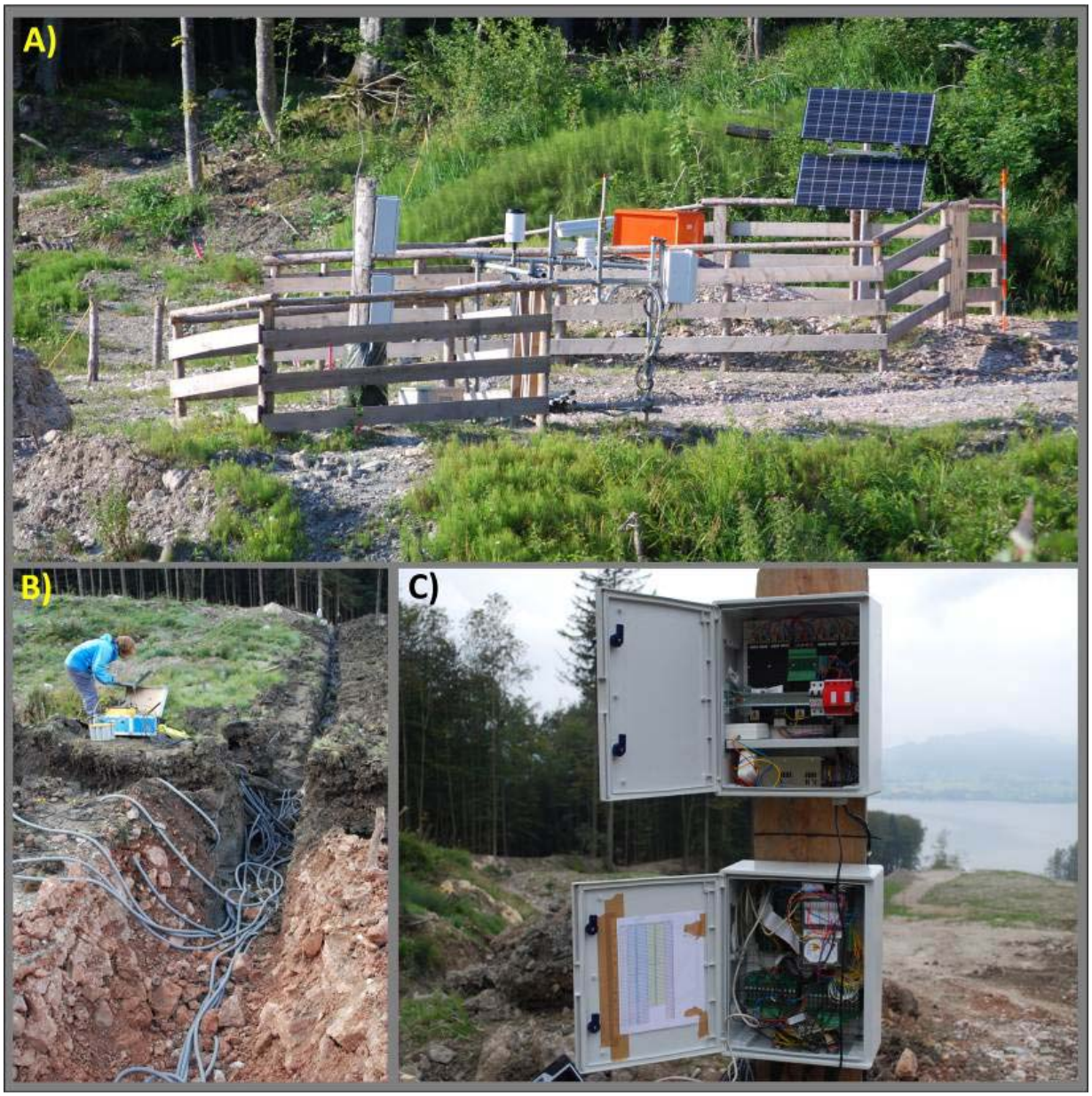

Figure 17. GEOMON4D instrument at the Gschliefgraben site: A) the control panel and the central unit were placed close to crossing of both monitoring profiles and close to the D.M.S. automatic inclinometer; B) the electrodes and cables were buried up to 1 m below the ground surface to protect them against major meteorological and mechanical circumstances; C) general appearance of the control unit (Photo by: Ivo Baron 2009 and 2010).

To define correlation between geoelectric anomalies and the triggering of movements, an innovative multiparametric monitoring system of stability D.M.S. (Differential Monitoring of Stability; Centro Servizi di Geoingegneria, Italy) was implemented at the crossing point of the GEOMON^{4D} profiles. The D.M.S. tool measures displacements in 2 directions with high accuracy (both horizontal and vertical at all the prefixed depths), piezometric ground-water level and soil temperature up to depths of 26 m below the ground-surface. Thus it allows the complex analysis of the dynamics of mass movement, e.g. deformation analysis, displacement, velocity, acceleration, and depth of failure or piezometric variations (FOGLINO et al., 2006).

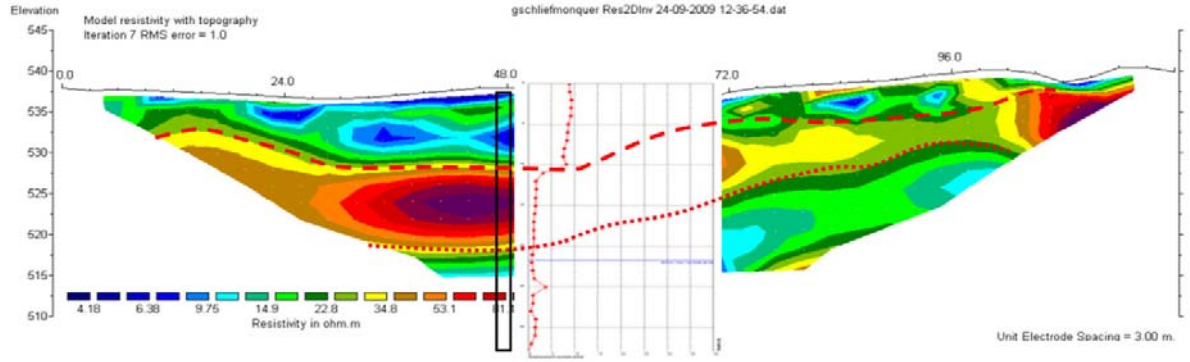

Figure 18. Correlation of resistivity layers with sliding surfaces determined by a permanent inclinometer (red curve) in the area of Gschliefgraben

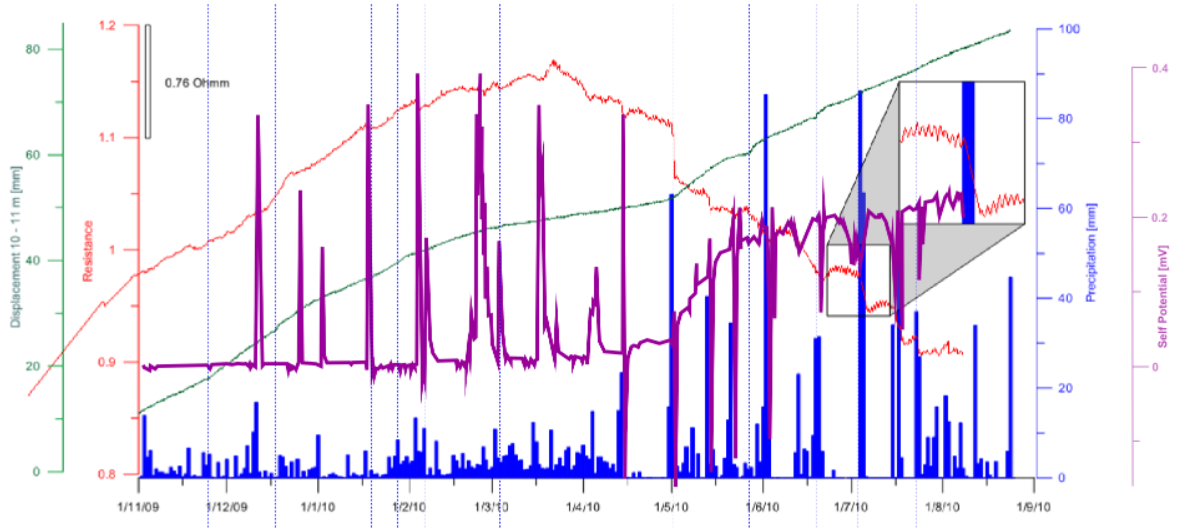

Figure 19. Results of monitoring at the landslide of Gschliefgraben in the period of November 2009 till July 2010: precipitation (blue), cumulative displacement (green), normalised electrical resistance (red; configuration 108-120-111-114), and normalised self-potential (purple). Moments of movement acceleration are marked by vertical dashed lines.

The preliminary results from the first year (Figs. 18 and 19) clearly show the long term stability of geoelectrical parameters and their response to changes in the hydrological system of the subsurface. They showed that intense rainfalls had a direct and immediate impact without any delay on the displacement and resistivity pattern causing very small, but clearly identifiable changes in both parameters.

References:

Baroň I., Supper R., Moser G., Gasperl W., 2010. Distinct topographic changes of an earthflow system at Gschliefgraben (Gmunden, Upper Austria) recorded by Differential Airborne Laser Scanning. – In. Krizek et al. (Eds): Geomorfologicky sbornik 9: 4, Charles University, Prague. ISBN: 978-80-86561-32-5

Baroň I., Supper R., Moser G., Gasperl W., 2010. Application of Differential Airborne Laser Scan for effective landslide inventory mapping and activity assessment in forested areas. – Geophysical Research Abstracts 12, EGU2010-4649-1, EGU General Assembly 2010

Foglino L., Lovisolo M., Della Giusta A., 2006. Contribution of DMS monitoring systems in the analysis of slide micro-movements for early warning management, risk assessment and evaluation of mitigating actions, Geophysical Research Abstracts, Vol. 8, 06122.

Egger H., Andorfer G., Braunstingl R., Fellner D., Friedel W., van Husen D., Jaritz W., Kleberger J., Mandl G., Müller J., Prey S., Schäffer G., Schneider J., Winkler K., 1996. Geologische Karte der Republik Österreich 1:50,000 (Geological Map of Austria) – Sheet 66 Gmunden. – Verlag den Geologischen Bundesanstalt, Wien.

Egger H, van Husen D., Frik G., Kohl H., Moser M., Moshammer B., Pavuza R., Prey S., Rogl Ch., Rupp Ch., Schermaier A., Schindlmayr A., Traindl H., 2007. Geologische Karte der Republik Österreich 1:50,000 (Geological Map of Austria) – Sheet 67 Grünau im Almtal. – Verlag den Geologischen Bundesanstalt, Wien.

Marschallinger R., Eichkitz C., Gruber H., Heibl K., 2009. The Gschliefgraben Landslide (Austria): A Remediation Approach involving Torrent and Avalanche Control, Geology, Geophysics, Geotechnics and Geoinformatics. – Austrian Journal of Earth Sciences, 102 (2): 36-51.

Moser G., et al., 2009. Großhangbewegung Gschliefgraben – Fachübergreifender Synthese-Bericht. – MS. Final report (in German). Moser/Jaritz and Wildbach und Lawinenverbauung. Gmunden, 329 pp.

Motschka K., 2001. Aerogeophysics in Austria. Bulletin of the Geological Survey of Japan Vol. 52 No. 2/3, pp. 83–88, Tsukuba, Japan.

Millahn K. et al., 2007: Geophysik im Gschliefgraben, ISDR, GdE 2004-2007. –MS. Final Report. Austrian Academy of Sciences and Leoben Montanistic University, 137 pp.

Niesner E., Weidinger J.T., 2008: Investigation of a historic and recent landslide area in Ultrahelvetic sediments at the northern boundary of the Alps (Austria) by ERT measurements. –The Leading Edge, SPECIAL SECTION: Near-surface geophysics, November 2008: 1498–1509.

Supper R., Baroň I., Jochum B, Ita A., Winkler E., Motschka K., Moser G., 2010a. Airborne Geophysics and Geoelectric and Inclinometric Monitoring at the Gschliefgraben Landslide. – In: Supper R., Baron I. (Eds.), 2010: Landslide Monitoring Technologies & Early Warning Systems – Current Research and Perspectives for the Future. – Book of Extended Abstracts. Open Workshop within the frame of the EU FP7 "SafeLand" Project, February 24th, 2010, Vienna, Berichte der Geologischen Bundesanstalt 82: 52-58.

Supper R., Baroň I., Ita A., Winkler E., Jochum J., Motschka K., 2010b. Airborne Geophysical Survey and Innovative Landslide Monitoring at Gschliefgraben, Austria. – Near Surface 2010, 16th European Meeting of Environmental and Engineering Geophysics, September 6-8, 2010, Zürich, Switzerland, CD Conference Proceedings.

Weidinger J.T., 2009: Das Gschliefgraben-Rutschgebiet am Traunsee-Ostufer (Gmunden/OÖ)-Ein Jahrtausende altes Spannungsfeld zwischen Mensch und Natur. –Jahrbuch der Geologischen Bundesanstalt 149 (1): 195-206.